AGU PUBLICATIONS

JGR

Journal of Geophysical Research: Atmospheres

RESEARCH ARTICLE
10.1002/2017JD026948

On the aliasing of the solar cycle in the lower stratospheric tropical temperature

Ales Kuchar[1,2], William T. Ball[2,3], Eugene V. Rozanov[2,3], Andrea Stenke[2], Laura Revell[2,4], Jiri Miksovsky[1], Petr Pisoft[1], and Thomas Peter[2]

[1]Department of Atmospheric Physics, Faculty of Mathematics and Physics, Charles University, Prague, Czech Republic, [2]Institute for Atmospheric and Climate Science, ETH Zurich, Zurich, Switzerland, [3]Physikalisch-Meteorologisches Observatorium Davos and World Radiation Center, Davos, Switzerland, [4]Bodeker Scientific, Christchurch, New Zealand

Key Points:
- Validation of the tropical stratospheric temperature response to the 11 year solar cycle (SC) in SOCOLv3 CCM
- Volcanic aliasing in the solar cycle attribution is quantified
- Reduced volcanic aliasing of the SC temperature response in the tropical lower stratosphere when the CMIP6 volcanic forcing is used

Correspondence to:
A. Kuchar,
kuchara@mbox.troja.mff.cuni.cz

Citation:
Kuchar, A., W. T. Ball, E. V. Rozanov, A. Stenke, L. Revell, J. Miksovsky, P. Pisoft, and T. Peter (2017), On the aliasing of the solar cycle in the lower stratospheric tropical temperature, *J. Geophys. Res. Atmos.*, *122*, 9076–9093, doi:10.1002/2017JD026948.

Received 11 APR 2017
Accepted 17 JUL 2017
Accepted article online 21 JUL 2017
Published online 6 SEP 2017

Abstract The double-peaked response of the tropical stratospheric temperature profile to the 11 year solar cycle (SC) has been well documented. However, there are concerns about the origin of the lower peak due to potential aliasing with volcanic eruptions or the El Niño–Southern Oscillation (ENSO) detected using multiple linear regression analysis. We confirm the aliasing using the results of the chemistry-climate model (CCM) SOCOLv3 obtained in the framework of the International Global Atmospheric Chemisty/Stratosphere-troposphere Processes And their Role in Climate Chemistry-Climate Model Initiative phase 1. We further show that even without major volcanic eruptions included in transient simulations, the lower stratospheric response exhibits a residual peak when historical sea surface temperatures (SSTs)/sea ice coverage (SIC) are used. Only the use of climatological SSTs/SICs in addition to background stratospheric aerosols removes volcanic and ENSO signals and results in an almost complete disappearance of the modeled solar signal in the lower stratospheric temperature. We demonstrate that the choice of temporal subperiod considered for the regression analysis has a large impact on the estimated profile signal in the lower stratosphere: at least 45 consecutive years are needed to avoid the large aliasing effect of SC maxima with volcanic eruptions in 1982 and 1991 in historical simulations, reanalyses, and observations. The application of volcanic forcing compiled for phase 6 of the Coupled Model Intercomparison Project (CMIP6) in the CCM SOCOLv3 reduces the warming overestimation in the tropical lower stratosphere and the volcanic aliasing of the temperature response to the SC, although it does not eliminate it completely.

1. Introduction

The influence of the 11 year solar cycle (SC) on reanalysis temperature data [*Frame and Gray*, 2010; *Mitchell et al.*, 2015a] or ozone observations [*Hood and Soukharev*, 2012] has been well documented. The solar cycle is often attributed using multiple linear regression analysis. In the tropics, the response consists of statistically significant warming and ozone increases in the upper (~1 hPa) and lower (~50 hPa) stratosphere, but with a minimum between (~10 hPa). Several transient Chemistry-Climate Model (CCM) simulations have partially reproduced the observed double-peaked temperature and ozone responses [*Egorova et al.*, 2004; *Austin et al.*, 2008]. However, there are concerns that the origin of the lower peak is due to potential aliasing of the solar cycle with El Niño–Southern Oscillation (ENSO) events [*Marsh and Garcia*, 2007] or volcanic eruptions [*Chiodo et al.*, 2014]. *Marsh et al.* [2007] also demonstrated that the solar cycle response from time slice simulations with fixed solar maximum or minimum forcings is very similar to the solar cycle response in transient simulations without a volcanic forcing and with variable sea surface temperature, for the period 1950–2003. However, for 1979–2003 the solar signal detected in transient simulations differs significantly from the signal simulated in time slice simulations with fixed solar maximum or minimum conditions. This difference already indicates a possible aliasing from using such a short (~2 cycles long) record.

It has been hypothesized that the lower stratospheric anomaly is caused by reduced upwelling at low latitudes, i.e., the Brewer-Dobson circulation (BDC) is weaker during solar maxima [*Kodera and Kuroda*, 2002; *Hood and Soukharev*, 2012]. These mechanisms—thought to be driven by the UV-induced changes in the upper stratosphere propagating downward ("top-down" mechanism) or by the non-UV-induced changes generated near the surface propagating upward ("bottom-up" mechanism) [*Gray et al.*, 2010]—are expected to

be particularly pronounced during the boreal winter when wave forcing is most active. *Muthers et al.* [2016] found a weak positive relationship between the 11 year solar cycle and age of air (a descriptive variable of the transport time, related to the BDC) when using the coupled atmosphere-ocean-chemistry-climate model SOCOL-MPIOM. Furthermore, other processes, such as the quasi-biennial oscillation (QBO), ENSO, and volcanic eruptions, must also be taken into account.

While the influence of the QBO on the solar signal in this region has been discussed elsewhere [e.g., *Lee and Smith*, 2003; *Smith and Matthes*, 2008; *Matthes et al.*, 2013], we focus here on variability in the tropical lower stratosphere (TLS) caused by ENSO and volcanic eruptions. Positive ENSO events (El Niño) cause a negative temperature anomaly at 50 hPa over the equator, whereas an opposite temperature response was detected in the case of volcanic eruptions [*Mitchell et al.*, 2015a; *Fujiwara et al.*, 2015].

It is important to point out that previous attribution studies differ in terms of regressors used, their time lag, and treatment of regression residuals. The choice of the applied regression can lead to different, even incorrect, interpretation of results. Two considerations should be made to properly attribute the signal through multiple linear regression (MLR). The first is to avoid the effect of autocorrelation of residuals, which could bias the variances of the ordinary least squares (OLS) estimates for the regression coefficients—the OLS estimates are still unbiased in the presence of residual autocorrelations, though inefficient [*Thejll and Schmith*, 2005]. The second is to account for, or eliminate, possible aliasing (multicollinearity) of regressors. Both of these are addressed in our analysis.

Mitchell et al. [2015b] assessed the 11 year SC in phase 5 of the Coupled Model Intercomparison Project (CMIP5) historical simulations, reporting that the signal in TLS temperature depends on the length of the analysis period. They pointed out that the strongest solar signal is found in the 1979–2005 period and acknowledged the possibility of aliasing effects. These have been already addressed by *Marsh and Garcia* [2007] and *Chiodo et al.* [2014] who suggested that the period covered by satellite measurements (1979 to present) is insufficient for solar signal detection by MLR due to contamination by ENSO events and volcanic eruptions, respectively. Thus, identification of a period from which a robust solar signal could be detected, i.e., separated from other phenomena influencing the lower stratospheric variability, is required. Furthermore, *Chiodo et al.* [2014] used CCM WACCMv3.5, which heavily overestimates the stratospheric warming after the Mount Pinatubo by ~3.5 K). In fact, this overestimated warming may enhance aliasing effects. Therefore, different models not suffering this discrepancy should also be used.

The paper is arranged as follows. First, we introduce our model experiments using the SOCOL (SOlar Climate Ozone Links) CCM (section 2.1), meteorological reanalysis and observational data sets used for model evaluation (section 2.2), and methodology based on MLR (section 3). Second, we validate the SOCOL CCM against observational and reanalysis records in terms of the temperature response to the SC and volcanic eruptions. By using CCM sensitivity simulations, we explain and quantify how the solar signal in the TLS was affected by volcanic eruptions and ENSO events during the past 50 years (section 4.1). In section 4.2, we show how the amplitude of the signal depends on the period and methodology applied in the regression analysis. Furthermore, we provide an elegant statistical explanation of the solar signal misattribution when using MLR, and then we reiterate that consideration of autoregressive (AR) components in MLR analysis is essential also that higher AR orders may be relevant for the lower stratosphere. Conclusions are presented in section 5.

2. Data and Models

2.1. Model Simulations

To carry out the model sensitivity simulations, we use version 3 of the SOCOL CCM [*Stenke et al.*, 2013], which is composed of the general circulation model MA-ECHAM-5 [*Manzini et al.*, 2006] and the chemistry part of the atmospheric chemistry transport model MEZON [*Egorova et al.*, 2003]. Our model experiments were performed with T42 horizontal resolution (grid cell sizes correspond to approximately 2.8° × 2.8°) and 39 vertical levels between the Earth's surface and 0.01 hPa (~80 km). The model setup is not able to simulate the QBO spontaneously, so equatorial stratospheric winds between 20°S and 20°N and from 90 hPa to 3 hPa have been relaxed toward observed wind [*Giorgetta et al.*, 2006; *Stenke et al.*, 2013].

The reference simulation (REF-C1) is part of the Chemistry-Climate Model Initiative (CCMI) activity [*Eyring et al.*, 2014; *Revell et al.*, 2015; *Morgenstern et al.*, 2017]. REF-C1 was forced by boundary conditions specified from observations, i.e., observed sea surface temperatures (SST) and sea ice concentrations (SIC) (see Table 1),

Table 1. Description of Model Simulations[a]

Simulation	Simulated Period	SST/SIC	Volcanic Forcing	# of Ensemble Members
REF-C1	1960–2009	Hadley record	√ (CCMI)	3
REF-C1-q	1961–2009	Hadley record	×	3
REF-C1-q-clim	1961–2009	Hadley climatology with respect to 1960–2009	×	3
REF-C1-CMIP6aer (Mt. Agung)	1960–1965	Hadley record	√ (CMIP6)	3
REF-C1-CMIP6aer (Mt. Pinatubo)	1986–2005	Hadley record	√ (CMIP6)	5

[a]Simulations correspond to the CCMI REF-C1 scenario [*Morgenstern et al.*, 2017]; volcanically quiescent variants are denoted by "q"; simulations without historical variability in sea surface temperature and sea ice coverage (SST/SIC) are denoted by "clim," i.e., climatology.

greenhouse gas concentrations, ozone depleting substances, tropospheric emissions, and volcanic and tropospheric aerosols. The Naval Research Laboratory Solar Spectral Irradiance (NRLSSI) model was used to calculate solar irradiance forcing [*Lean et al.*, 2005], which was also used in previous CCMVal [*CCMVal*, 2010] and CMIP5 [*Hood et al.*, 2015; *Mitchell et al.*, 2015b] experiments. One such simulation (REF-C1) was performed with a 10 year spin-up period starting in 1950.

To investigate the role of volcanic eruptions or SST/SIC boundary conditions on the solar cycle signal, additional sensitivity simulations were performed, covering the period 1961–2009. REF-C1-q was performed to simulate volcanically *quiescent* conditions; its setup was identical to REF-C1 but without any forcing by volcanic aerosols (i.e., only background stratospheric aerosols from year 2000 were used for the entire simulation). However, REF-C1-q may still contain volcanic perturbations embedded in the prescribed, historical SST/SIC. In order to avoid volcanic, and additional SST/SIC impacts such as ENSO, on stratospheric variability, we performed another simulation, termed REF-C1-q-clim, using a monthly *climatology* of SST/SIC values from 1960 to 2009. REF-C1-q and REF-C1-q-clim consist of three transient ensemble runs with slightly different initial CO_2 concentrations during the first simulated month (about ±0.5%).

Furthermore, we investigate the influence of prescribed volcanic forcing on the temperature in the TLS region. Therefore, additional sensitivity simulations were performed, covering the Mount Pinatubo and Agung eruption periods using the new CMIP6 volcanic forcing [*Luo*, 2016] instead of the original volcanic forcing used in the CCMI framework [*Luo*, 2013]. All simulations are summarized in Table 1.

2.2. Data Sets Used for Model Evaluation

To validate our SOCOL simulations, we use two reanalyses: Modern-Era Retrospective Analysis for Research and Applications-2 (MERRA2) [*Koster et al.*, 2015] and Japanese 25-year Reanalysis (JRA-55) [*Ebita et al.*, 2011]. The latter is used because it covers the whole simulated period (available from 1958 to present). Furthermore, we use merged satellite temperature measurements from the NOAA Stratospheric Sounding Unit (SSU) and Advanced Microwave Sounding Unit-A (AMSU-A) [*Zou and Qian*, 2016] for the period 1980–2009. SSU temperature time series are represented by its three channels whose weighting functions peak at pressures of approximately 14.6, 4.6, and 1.9 hPa [*Chen et al.*, 2011]. For the TLS validation, AMSU satellite temperature measurements [*Mears and Wentz*, 2009] are included (at a pressure level of approximately 83 hPa) together with radiosonde data set HadAT2 [*Thorne et al.*, 2005].

3. Regression Analysis

To detect variability and changes due to external climate factors, including the 11 year solar cycle, we have used an attribution method based on the MLR analysis applied by *Kuchar et al.* [2015]. This regression model (Greek letters represent regression coefficients.) is applied to a monthly deseasonalized time series Y, reconstructing it as a function of time t:

$$\begin{aligned} Y(t) = \alpha + \beta \mathrm{SAD}(t) + \gamma \mathrm{F}_{10.7}(t) \\ + \delta_1 \mathrm{QBO}_1(t) + \delta_2 \mathrm{QBO}_2(t) + \epsilon \mathrm{ENSO}(t) \\ + \zeta \mathrm{TREND}(t) + e(t). \end{aligned} \quad (1)$$

The regression model uses predictors representing climate forming factors that have an impact on middle atmosphere conditions, i.e., the 10.7 cm radio flux as a solar proxy (The data set was acquired from

Dominion Radio Astrophysical Observatory in Penticton, Canada. Follow this link: ftp://ftp.geolab.nrcan.gc.ca/data/solar_flux/monthly_averages/.) ($F_{10.7}$), globally averaged aerosol surface area density at 54 hPa (SAD) for volcanic eruptions, the ENSO3.4 index representing ENSO variability, and two proxies for the quasi-biennial oscillation (QBO). Values for SAD in equation (1) have been obtained from the CCMI data set of *Luo* [2013] [see also *Arfeuille et al.*, 2013]. The ENSO3.4 index (averaged sea surface temperature anomaly in the region bounded by 5°N to 5°S and from 170°W to 120°W) is extracted from the HadISST data set [*Rayner et al.*, 2003], which was also used as the SST/SIC boundary condition for our simulations. REF-C1-q and REF-C1-q-clim were both evaluated without volcanic regressors and the latter without an ENSO regressor. After assessing the structure of the regression residuals, there is no indication of bias from the residuals resulting from the absence of an important missing regressor for our regression analysis setups.

The QBO proxies were extracted by principal component analysis from the residuals of our regression model excluding QBO regressors and residual modeling following *Frame and Gray* [2010]. The zonal mean of the model's zonal winds, between 10°S and 10°N and from 50 hPa to 10 hPa, is used as an input for extraction of QBO proxies.

The linear regression is based on estimating regression coefficients by least squares minimization. To avoid autocorrelation of residuals $e(t)$, an iterative algorithm was used to model residuals as a second-order autoregressive process (generally termed AR2). Statistical significance at 2σ confidence intervals computed by t test is presented. We obtained similar results using a more robust bootstrap method based on 5000 samples using our regression model with AR2 to account for autocorrelation of residuals (not shown).

Furthermore, we also used MLR to derive the tropical temperature response to the eruptions of Mount Agung, El Chichón, and Mount Pinatubo. The temperature response for each eruption was extracted as the difference between 12 month averaged $R(t)$ after each eruption and the 36 month averaged $R(t)$ before each eruption (following *Fujiwara et al.* [2015]). $R(t)$ is the residual of our regression model (1) when volcanic regressors and residual modeling (AR2) were not used.

To facilitate the reproducibility of results within the solar-climate modeling community, where MLR is widely used, and to account for possible differences in regression approaches, we developed an MLR-based tool called *X regression* [*Kuchar*, 2016]. An accompanying Github repository has been created to document the methodological approach used in this paper and to accelerate future activities focused on solar cycle attribution and validation of climate models. This tool is based on the Python open-source software library *statsmodels* [*Seabold and Perktold*, 2010] coupled with *xarray* [*Hoyer and Hamman*, 2017].

4. Results

To introduce the aliasing within the TLS, Figure 1a shows how two major volcanic eruptions, El Chichón in 1982 and Mount Pinatubo in 1991, represented by time series of globally averaged SAD at 54 hPa, are aligned with the descending phase of solar maxima 21 and 22 represented by time series of 10.7 cm solar radio flux, respectively. Figure 1b provides a comparison of deseasonalized tropical temperature time series between SOCOL simulations and MERRA2 reanalysis at 50 hPa. The time series in Figure 1b highlights three important source of variability: the QBO, the long-term stratospheric cooling trend from 1960 up to 2000, and several warming peaks associated with volcanic eruptions. It is also apparent that the REF-C1 simulation overestimates the tropical temperature response in the TLS to Mount Pinatubo eruption as compared to MERRA2 reanalysis. This overestimation disappears in the REF-C1-CMIP6aer ensemble due to different gap-filling procedures used to compile the CCMI and CMIP6 stratospheric aerosol data sets when the lower stratosphere is too optically thick following the eruption for occultation instruments on board satellites to measure [*Revell et al.*, 2017] (see also enlarged Figures 1c–1e for Mount Agung, El Chichón, and Mount Pinatubo volcanic eruptions, respectively).

4.1. Tropical Temperature Response to the SC

Figure 2a shows the modeled solar cycle maximum to minimum (The signal is expressed as the average difference between the solar maxima and minima in the period 1979–2013, i.e., normalized by $F_{10.7} = 126.6$ solar flux units.) (see Figure 1a) zonally averaged temperature response between 25°S and 25°N using monthly mean averages compared with MERRA2 and SSU. In Figure 2a the upper stratospheric response of REF-C1 (black line) peaking at 1.5 hPa agrees well with MERRA2 (shading) and, in particular, SSU (red error bars) estimates. A stronger signal in the reanalysis can be partly attributed to the existence of discontinuities in 1979,

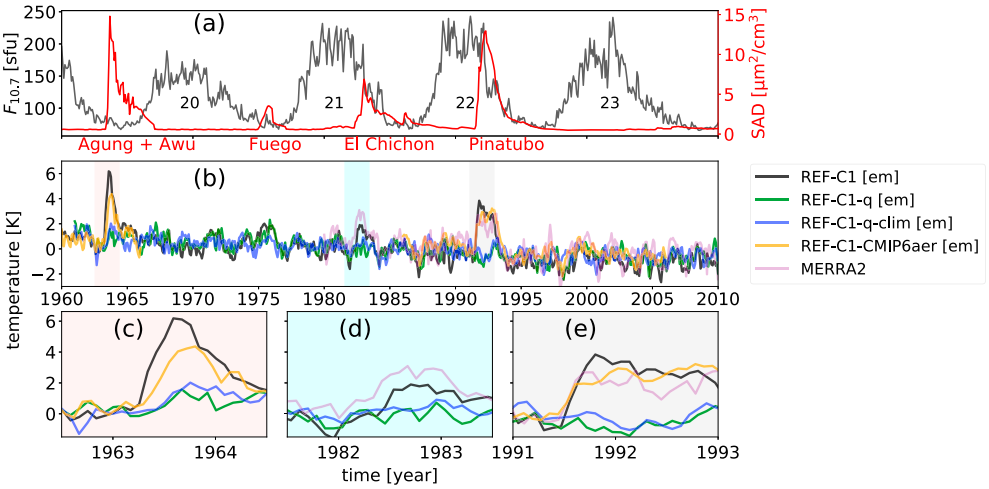

Figure 1. (a) Time series of 10.7 cm solar radio flux ($F_{10.7}$; black line) and globally averaged aerosol surface area density at 54 hPa (SAD; red line) from 1960 to 2009 used in CCMI simulations [*Luo*, 2013]. (b) Deseasonalized tropical temperature time series at 50 hPa for REF-C1 and REF-C1-CMIP6aer (all forcings, black and orange line), REF-C1-q (quiescent, i.e., without volcanic forcing, green line), REF-C1-q-clim (quiescent and replacing SST/SIC interannual variability by climatological values, blue line), and MERRA2 reanalysis (purple). Temperature time series from Figure 1b, Mount Agung, El Chichón, and Mount Pinatubo volcanic eruptions, are enlarged in Figures 1c–1e, respectively.

1985, and 1998 as discussed by *McLandress et al.* [2014], coinciding with major changes in instrumentation or reanalysis procedure, particularly at 5 hPa and above, and also seen in ERA-Interim [*Dee et al.*, 2011; *Rienecker et al.*, 2011]. *Kuchar et al.* [2015] stated that the difference between the temperature response to the SC of non-adjusted and adjusted ERA-Interim data sets is about 0.2 K in the upper tropical stratosphere. Another reason for the difference between model results is that MERRA2 and SSU in the upper stratosphere may result from the use of the NRLSSI solar forcing [*Lean et al.*, 2005] used in CCMI, which gives a smaller temperature response in comparison to other forcings (see Figure 10 for SOCOL in *Ermolli et al.* [2013]). This is most likely related to the NRLSSI model's conservative SSI variability in the UV range in comparison with other SSI data sets. However, it is unlikely that using, e.g., the SATIRE SSI forcing [*Krivova et al.*, 2010; *Yeo et al.*, 2014] would change the temperature response so significantly [*Ball et al.*, 2014; *Matthes et al.*, 2016]. At ~15 hPa, REF-C1 shows a

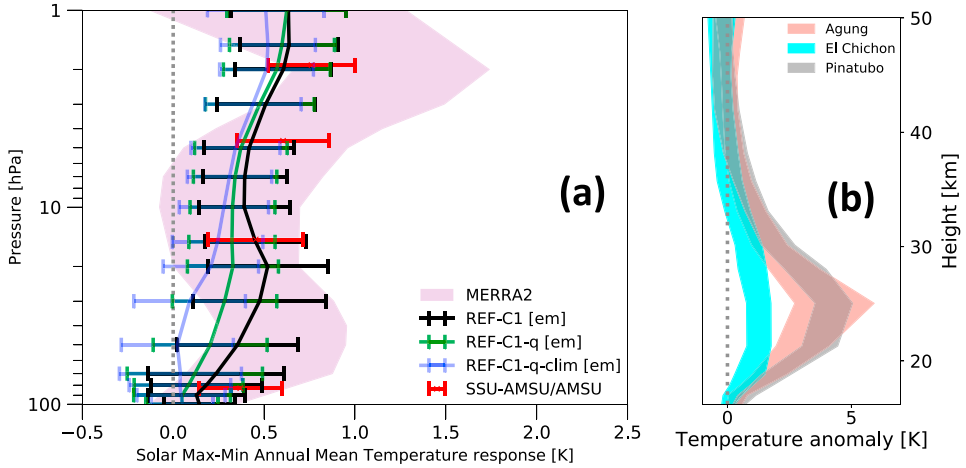

Figure 2. (a) Tropical (zonal mean between 25°S and 25°N) annual mean temperature response to solar variability, i.e., normalized regression coefficient γ from equation (1), over the period 1980–2009 in SOCOLv3 (ensemble mean (em) of REF-C1, REF-C1-q and REF-C1-q-clim), in comparison with MERRA2, SSU-AMSU, and AMSU. The signal is expressed as the average difference between solar maxima and minima in the period 1979–2013. Horizontal bars and shaded area (MERRA2): 95% confidence interval of γ coefficient in equation (1) (determined with AR2). (b) Tropical temperature response to the eruptions of Mount Agung (orange shading), El Chichón (cyan shading), and Mount Pinatubo (gray shading) in REF-C1 simulation. Error bars represent 95% confidence intervals for the difference in the means.

Table 2. Normalized Regression Coefficient γ (Unit: K) Values From Equation (1) and Figure 2a, Over the Period 1980–2009 in SOCOLv3 (REF-C1, Ensemble Mean (em) of REF-C1-q and REF-C1-q-clim), in Comparison With MERRA2 at Four Pressure Levels[a]

	Pressure Levels (hPa)			
	20	30	50	70
MERRA2	**0.35**	**0.52**	**0.58**	**0.47**
REF-C1 (em)	**0.52**	**0.48**	**0.35**	0.23
REF-C1-q (em)	**0.33**	0.28	0.20	0.12
REF-C1-q-clim (em)	0.21	0.09	0.02	0.04

[a]Values in bold denote statistical significance at 2σ confidence intervals computed by the *t* test.

similar response as SSU, and from 50 hPa downward REF-C1 is in good agreement with MERRA2 and AMSU. The double-peaked structure calculated using reanalysis data sets for the period starting in 1979 [e.g., *Frame and Gray*, 2010; *Mitchell et al.*, 2015a], observational data sets [*Randel et al.*, 2009; *Hood and Soukharev*, 2012], and also model transient simulations [e.g., *Austin et al.*, 2008; *Hood et al.*, 2015] is also found in the SOCOL reference simulation REF-C1 (black line in Figure 2a). While the SC detected in SOCOL peaks between 20 and 30 hPa (see Table 2), the SC detected in MERRA2 peaks between 40 and 50 hPa. The origin of this systematic difference is likely a result of using the CCMI volcanic forcing, and we discuss this further below.

In Figures 2a and 2b we show how attributed solar and volcanic effects overlap in the TLS. Figure 2b shows the tropical temperature response to the eruptions of Mount Agung, El Chichón, and Mount Pinatubo (following the procedure by *Fujiwara et al.* [2015], described in section 3). This suggests that aerosol heating can either mimic the solar signal, thus enhancing its amplitude, or cancel out the solar signal, thus decreasing its amplitude in the TLS.

The REF-C1 results provide a reference for the following sensitivity tests with slightly different boundary conditions. To estimate the direct impact of volcanic eruptions on the extraction of the solar cycle signal from the SOCOL model, we perform the same ensemble set as before, but with only background stratospheric aerosols included (REF-C1-q; green line in Figure 2a). Elimination of the volcanic aerosol in REF-C1-q leads to a weaker equatorial temperature response than in REF-C1 throughout the whole stratosphere and especially from 20 hPa downward; below 30 hPa the signal is not statistically different from zero. While the double-peaked structure in REF-C1-q is still apparent (a weak secondary maximum around 20 hPa), the lower stratospheric temperature shows a reduced response to the 11 year SC. Given that the only difference between REF-C1 and REF-C1-q is that the latter has no volcanic aerosol forcing, the implication is that the temperature response to the solar forcing is overestimated (almost doubled near 50 hPa) due to the volcanic aliasing in the solar signal. This confirms the conclusion of *Chiodo et al.* [2014] who used WACCMv3.5 — a model different to SOCOL, but overestimating the warming after Mount Pinatubo as well.

To completely eliminate any volcanic influence that may reach the stratosphere indirectly via a feedback response from the oceans, we performed a historical simulation similar to REF-C1-q, but with SST/SIC boundary conditions set to the climatology of the period, i.e., REF-C1-q-clim. The temperature response in the TLS attributed to solar forcing is further reduced in the REF-C1-q-clim simulation with climatological SST/SIC boundary conditions (blue line in Figure 2a). The TLS temperature responses for all our simulations and MERRA2 regarding TLS is listed in Table 2.

The signal attributed to the SC is reduced by 44% and 50% at 50 and 70 hPa, respectively, when volcanoes are quiescent; switching off SST/SIC interannual variability leads to a 94% reduction of the mean SC signal at 50 hPa (0.36 K versus 0.02 K in Table 2). This highlights that SST/SIC interannual variability for simulating the secondary maximum in the TLS may be crucial. In addition to REF-C1-q, REF-C1-q-clim aims to avoid the possibility of volcanic signal artifacts being carried via SST/SIC in the HadISST data [*Gray et al.*, 2013], or even other types of SST/SIC interannual variability that could contain ENSO variability or imprints of solar, or other decadal-like, oscillation (e.g., Pacific Decadal Oscillation) [*Wang et al.*, 2016]. Therefore, we hypothesize that since the solar signal above 10 hPa attributed from REF-C1-q-clim is essentially the same as in REF-C1, it represents the top-down mechanism only [*Gray et al.*, 2010], i.e., a separation from a bottom-up mechanism

and aliasing with volcanic eruptions. However, top-down and bottom-up mechanisms are not necessarily mutually exclusive since UV-induced changes in the upper stratosphere propagating downward can partly drive the troposphere-ocean response, in addition to direct forcing by total solar irradiance variations at the surface [*Hood and Soukharev*, 2012].

Note that the results in Table 2 for REF-C1-q and REF-C1-q-clim are insensitive to when our full regression model (discussed in section 3) was applied with all regressors or when we intentionally omitted the volcanic predictor, or volcanic and ENSO predictors, in the original regression analysis for REF-C1-q or REF-C1-q-clim, respectively. However, the results for REF-C1 are sensitive to removing the volcanic predictor, in particular. This confirms that there is the physical aliasing in the time series between the SC and other variability drivers missing from our idealized simulations REF-C1-q and REF-C1-q-clim.

Further evidence to support these results comes from looking at the global wavelet power spectra [*Torrence and Compo*, 1998], obtained for three pressure levels in the tropical stratosphere. In Figure 3 we identify the occurrence of an 11 year SC periodicity in our simulations' time series. The spectra are in agreement in the upper stratosphere (Figure 3a; ~1 hPa) for all our simulations that show a decadal periodicity that we attribute to solar variability, and a periodicity related to the QBO (~28 months). At lower pressure levels (20 hPa; Figure 3b), we can see that the power of these two periodic signals is enhanced (note different *y* axis scale) in REF-C1, where decadal variability is increased due an approximate decade of separation between volcanic eruptions (Figure 1a). We confirm this by removing 3 years following the Mount Pinatubo eruption (compare black lines in Figure 3). QBO periodicity is enhanced especially during the Mount Agung and Mount Pinatubo eruptions (as indicated by the local wavelet amplitude — not shown). This enhancement may come from the fact that diabatic warming in the TLS caused by a volcanic eruption masks potential warming or cooling induced by the QBO via adiabatic heating or heating associated with downward or upward vertical motion, respectively. Down to 20 hPa we can also see that the solar (decadal-like) signal was almost identical for our two sensitivity simulations REF-C1-q and REF-C1-q-clim (see green and blue lines in Figure 2a). The same fact is valid for their global power spectra in Figure 3b. At 50 hPa (Figure 3c) we can see pronounced differences for periods longer than normal for the QBO between REF-C1-q and REF-C1-q-clim, i.e., decadal and ENSO-like periods [see, e.g., *Torrence and Compo*, 1998] were filtered out in the case of REF-C1-q-clim. This supports our finding that the solar signal was reduced to almost zero at this level in the REF-C1-q-clim simulation (Figure 2a). While the QBO-matched periodicity is statistically significant at all pressure levels in all simulations, i.e., the global wavelet power is above the 95% confidence interval of the corresponding mean red noise spectrum, the decadal-like periodicity is significant only at 1 hPa in all simulations. Furthermore, while the decadal-like periodicity in REF-C1 is significant at all shown pressure levels, the global wavelet power of this periodicity in REF-C1-q exceeds the mean red noise spectrum power only down to 20 hPa (not shown).

Before proceeding further, we briefly digress from the SC discussion to deal with an important question related to the sensitivity of the volcanic signal to the model configuration or to the prescribed aerosol boundary conditions, since the temperature response to a volcanic eruption, and aliasing with the SC, potentially depends on both of these factors. Furthermore, it can affect the magnitude of the volcanic aliasing of the temperature response to the SC in the TLS. Figure 4 compares observational (HadAT2) and reanalysis (MERRA2 and JRA-55) data sets with SOCOL simulations. Using time series' comparison in Figures 1b–1e, we have already shown that REF-C1 overestimates the warming after the Mount Agung and Pinatubo eruptions in the TLS (see gray bar in Figure 4). The warming after the Pinatubo eruption is about 1.55 and 1.50 K higher than in MERRA2 reanalysis (purple bar) and HadAT2 radiosonde data (light blue bar), respectively. The simulated warming in REF-C1 after the Mount Agung eruption seems to be biased in terms of mean values with respect to HadAT2 and JRA-55 (about 1.40 K), though with high uncertainty. On the other hand, the warming in REF-C1 after El Chichón is slightly underestimated by 0.31 K but is still within the range of confidence intervals. Simulated temperature anomalies in SOCOLv3 REF-C1 are overestimated because there is substantially more aerosol loading in the TLS following the Mount Pinatubo eruption in the CCMI aerosol data set cf. the CMIP6 data set [*Revell et al.*, 2017]. Therefore, the magnitude of the volcanic aliasing of the solar signal in the TLS may be overestimated as well.

To examine the excessive model response to volcanic aerosols, we performed additional sensitivity simulations based on the REF-C1 setup, with five ensemble members covering the Mount Pinatubo and Agung eruption periods, employing the volcanic forcing prepared for CMIP6 simulations (see orange colored bar in Figure 4). For more details about the CMIP6 volcanic forcing based on the SAGE-3λ algorithm [*Luo*, 2016],

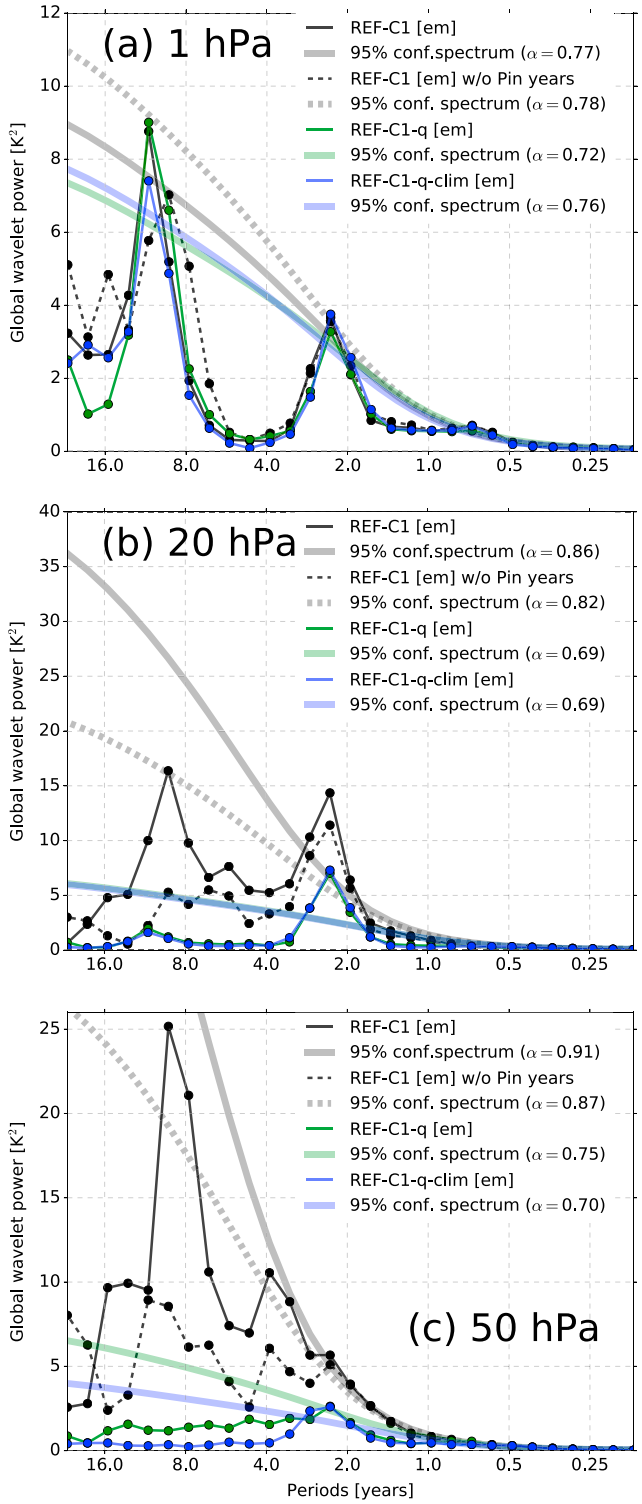

Figure 3. Global wavelet power spectra using a Morlet wavelet with the parameters (see details in *Torrence and Compo* [1998]): wave number $\omega_0 = 6$, $\delta t = 1/12$years, $s_0 = 2\delta t$, $\delta j = 0.25$, and $J = 7/\mathrm{d}j$; applied on tropical temperature detrended time series over the simulated period of particular simulation at (a) 1 hPa, (b) 20 hPa, and (c) 50 hPa for REF-C1 (black and solid lines with points), REF-C1 with 1991, 1992, and 1993 years excluded (black and dashed lines), REF-C1-q (green and solid lines with points), and REF-C1-q-clim (blue and solid line with points) simulations. The wider and less intense lines (without points) represent the 95% confidence spectrum based on the mean red noise spectrum assuming a lag 1 α autoregressive process (AR1) of particular simulations denoted in the legend.

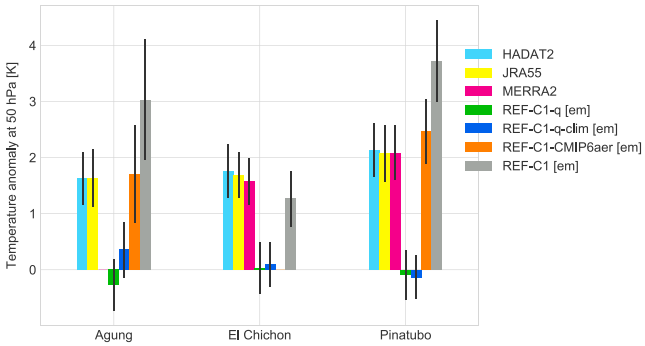

Figure 4. Comparison of tropical temperature responses to the eruptions of Mt. Agung, El Chichón, and Mount Pinatubo at 50 hPa between ensemble mean (em) of REF-C1 (gray bar), REF-C1 with the CMIP6 forcing (orange bar), REF-C1-q (blue bar), REF-C1-q-clim (green bar) and reanalyses MERRA2 (magenta bar) and JRA-55 (yellow bar), and radiosondes HadAT2 (light blue bar). Error bars represent 95% confidence intervals for the difference in those means.

see *Revell et al.* [2017]. Figure 4 shows that the tropical temperature response to both eruptions was reduced and is in agreement with reanalyses and HadAT2 data sets. However, this result needs to be confirmed for other CCMI models since this result holds only for SOCOLv3 and may not necessarily hold for other CCMI models.

Since the REF-C1 simulation with the CMIP6 volcanic forcing (REF-C1-CMIP6aer) did not show the overestimated warming after the Mount Pinatubo eruption in the TLS, we test whether this change affects the magnitude of the volcanic aliasing. Figure 5 shows an analogical analysis to Figure 2a, i.e., profiles of the tropical temperature response to the SC, but the period 1986–2005, the period over which we have available all five ensemble members of REF-C1-CMIP6aer. The temperature response to the SC in REF-C1-CMIP6aer reveals agreement in the upper stratosphere with other SOCOL simulations. From 3 hPa downward its profile starts to diverge—revealing an overall reduced response in comparison to the original REF-C1 simulation and much closer to MERRA2 between 10 and 30 hPa. To conclude, the REF-C1-CMIP6aer ensemble shows that when the overestimated warming due to volcanic aerosols in the TLS is reduced, the magnitude of the volcanic aliasing of the temperature response to the SC is reduced as well, albeit not eliminated completely.

To document how the systematic altitude shift in volcanic forcing may influence the systematic altitude shift in the solar signal. While the temperature response to the Mount Pinatubo volcanic eruption in REF-C1 peaks at 30 hPa, in MERRA2 it peaks at 40 hPa. This systematic shift may be a result of the CCMI volcanic forcing used:

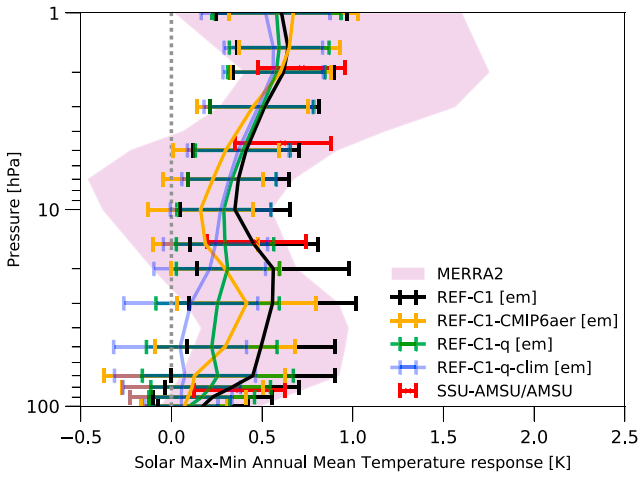

Figure 5. Tropical (zonal mean between 25°S and 25°N) annual mean temperature response to solar variability, i.e., normalized regression coefficient γ from equation (1), over the period 1986–2005 in SOCOLv3 (ensemble mean (em) of REF-C1, REF-C1 with the CMIP6 volcanic forcing, REF-C1-q and REF-C1-q-clim), in comparison with MERRA2, SSU-AMSU and AMSU. The signal is expressed as the average difference between solar maxima and minima in the period 1979–2013. Horizontal bars and shaded area (MERRA2): 95% confidence interval of γ coefficient (determined with AR2).

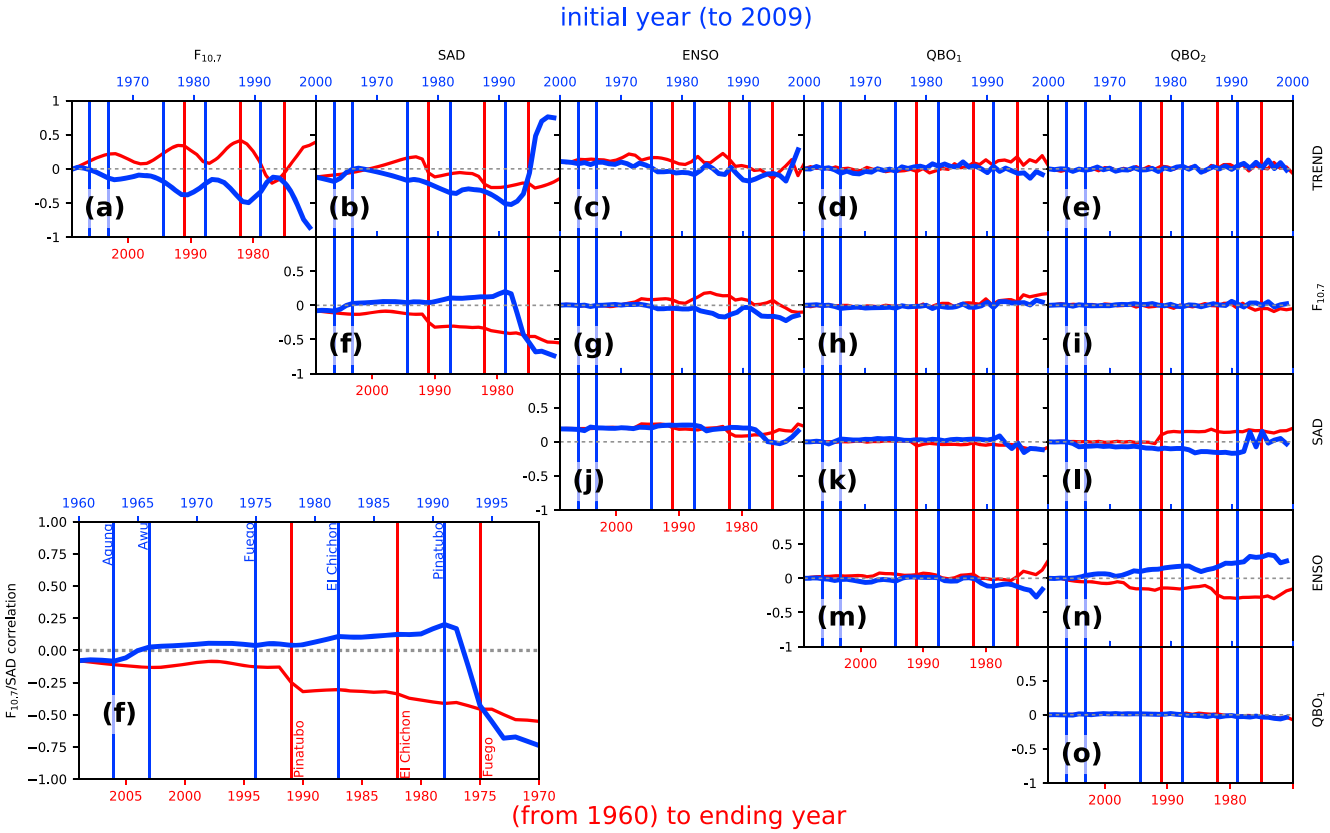

Figure 6. Correlation coefficients between all regressors. Blue: correlations from periods ending in the year 2009 and beginning in different starting years (indicated in time top axis). Red: correlations starting in the year 1960 closing in different ending years (indicated in the bottom axis). Vertical lines: eruptions of Mount Agung (1963), Mount Awu (1966), Mount Fuego (1974), El Chichón (1982), and Mount Pinatubo (1991). In the lower left corner the correlation plot between $F_{10.7}$ and SAD is enlarged for clarity. The statistical significance was computed by a test when regressors' autocorrelations were employed [*Bretherton et al.*, 1999]. Blue and red dots would indicate periods when p values < 0.05.

for example, zonally averaged (25°S–25°N) extinction coefficients within the infrared solar band (between 2380 nm and 4000 nm) reach a maximal height of 22.6 km (~35 hPa) on average during the first year after the Mount Pinatubo eruption, and it also leads to a systematic shift in the SC temperature response (see Figure 2a). In the TLS the solar signal in REF-C1-CMIP6aer peaks at 30 hPa, which is the last pressure level statistically different from zero. This documents a systematic shift in the solar signal detected in the TLS between REF-C1 with the CCMI volcanic forcing peaking at ~20 hPa and REF-C1 with the CMIP6 volcanic forcing peaking at ~30 hPa.

4.2. Effects of Aliasing (Multicollinearity) and Autocorrelated Residuals

In this subsection we examine a linear relationship between the regressors used in our attribution model equation (1) to reveal potential signs of aliasing between our explanatory variables. There is evidence that the alignment between the two major volcanic eruptions El Chichón and Mount Pinatubo with the descending phases of solar maxima is likely projected into the correlation between solar and volcanic proxies and therefore a change in the regression coefficients. However, similar alignment may also occur between solar activity and another regressor in our regression model equation (1). Therefore, in Figure 6 we illustrate the evolution of the correlation matrix between all regressors used in equation (1) for an expanding analysis period that starts between years 1960 and 1999 and ending in 2009 (blue line and top blue axis), or starting in 1960 and ending between 1970 and 2009 (red line and bottom red axis). Note that the correlations were not statistically different from zero when regressors' autocorrelations were employed in estimating the statistical significance using effective sample size [see *Bretherton et al.*, 1999, equation (31)].

The correlation between solar and volcanic proxies (see zoomed-in correlation plot in the lower left corner of Figure 6f) for the whole period 1960–2009 is slightly negative (far left values; ~ 0.1). After the blue curve, after Mount Agung eruption, the correlation increases and becomes positive by 1965. Following El Chichón,

the correlation reaches 0.1 and increases to 0.2 by the time of the Mount Pinatubo eruption. Afterward the correlation becomes negative. The negative correlation is persistent also when, instead of changing the initial year of our correlation analysis with fixed ending year 2009, we change the ending year with fixed initial year 1960 (red line and bottom axis in Figure 6). This is because Mount Agung and Awu eruptions occurred in a solar minimum between the solar maxima 19 and 20. Similarly, the negative correlation between 2000 and 2009 pertains to a period when increasing SAD values, caused by minor volcanic eruptions [*Vernier et al.*, 2011], coincide with the declining phase of the solar maximum 23.

While correlation values between solar and volcanic proxies mostly do not exceed 0.2 (except for a very short period after the Mount Pinatubo eruption), correlations between solar and trend proxies reach higher values and decrease as the start year is shifted back from 1999 to 1960 (red line), with an apparent solar cycle variation superimposed. Furthermore, we can see periods shorter than 1975–2009 revealing nonzero correlations between solar and ENSO proxies. This correlation sensitivity to initial and ending year of the analysis period should be taken into account when assessing whether such aliasing interferes with the attribution of the solar signal, as demonstrated in Figure 2a. Since the relationships between our regressors are sensitive to the time period considered, the regression coefficients are sensitive to the initial year of the analysis period as well.

To demonstrate the impact of the regressor aliasing for various data sets, we vary the length of the regression window with either a fixed initial year or an ending year for the tropical temperature response to the SC at 50 hPa, i.e., following the approach used by *Chiodo et al.* [2014]. The results are plotted as red error bars in Figures 7 and 8. In addition to SOCOL (Figures 7a–7c and 8a–8c) and MERRA2 (7e and 8e), we include the JRA-55 (7d and 8d), and HadAT2 (7f and 8f). The shortest period analyzed was 10 years, i.e., 1999–2009 or 1960–1970, respectively.

The REF-C1 temperature response (Figure 7a) is sensitive to the initial year of analysis in terms of both magnitude and statistical significance. By increasing the number of years considered in the analysis, the confidence interval becomes narrower and the response varies from near zero (from 1992 onward) to 0.5 K (1990–2009). However, when considering the whole period, i.e., 1960–2009, the temperature response converges to stable values that are not statistically different from zero. By "stability" we mean that the amplitude and confidence intervals stop varying with the initial year of analysis, which can be seen in Figure 7a for periods with an initial year earlier than 1975. Note that the REF-C1-q and REF-C1-q-clim temperature responses are never statistically different from zero in Figures 7b and 7c, respectively. The analysis with the regression window starting in 1960 and ending between 1970 and 2009 shows a similar tendency to stabilized values for longer periods where $F_{10.7}$ and SAD aliasing diminishes (see Figure 8). This corresponds to the correlation analysis in Figure 6f (red lines).

The evolution of the signal in REF-C1 (Figure 7a), starting from 1979, is similar to the signal in MERRA2 (Figure 7e) and JRA-55 (Figure 7d), i.e., the regression coefficients are inflated during periods when El Chichón and Mount Pinatubo eruptions are considered. It clearly resembles the shape (and evolution) of the correlation between solar and volcanic proxies in Figure 6f (blue line). The evolution of the signal in REF-C1-q (Figure 7b) reveals "bumps" in periods with initial years after 1975 and 1985, reminiscent of the evolution of the correlation between solar and ENSO proxies. This variation diminishes in REF-C1-q-clim (Figure 7c). On the other hand, the signals' stabilization effect in JRA-55 and HadAT2 is a bit shifted toward longer periods and they are still statistically significant even for the periods prior to 1980, similar to other reanalyses that have data available back to 1960, e.g., 20CR [*Compo et al.*, 2011] or National Centers for Environmental Prediction-1 [*Kalnay et al.*, 1996] (not shown). This corresponds to the fact that our simulations REF-C1 and REF-C1-q converge to positive values when periods shorter than 1960–1975 are analyzed in Figures 8a and 8b. On the other hand, JRA-55 and HadAT2 (Figures 8d and 8f) rather converge further to negative values for the same periods. However, they are not statistically different from zero for all cases. This indicates that the regressed solar variability is different in SOCOL simulations with prescribed SST/SIC interannual variation for the periods prior to 1975. Since REF-C1-q-clim (Figure 8c) does not reveal similar behavior for any period, we consider that this difference possibly stems from the underlying SST variability and its impact on the TLS region (see also green and blue lines in Figure 3c).

The misattribution of the solar signal detected by the linear regression has an elegant statistical explanation. The amplitude of the signal of one regressor is related to the presence of another regressor, so that the signal

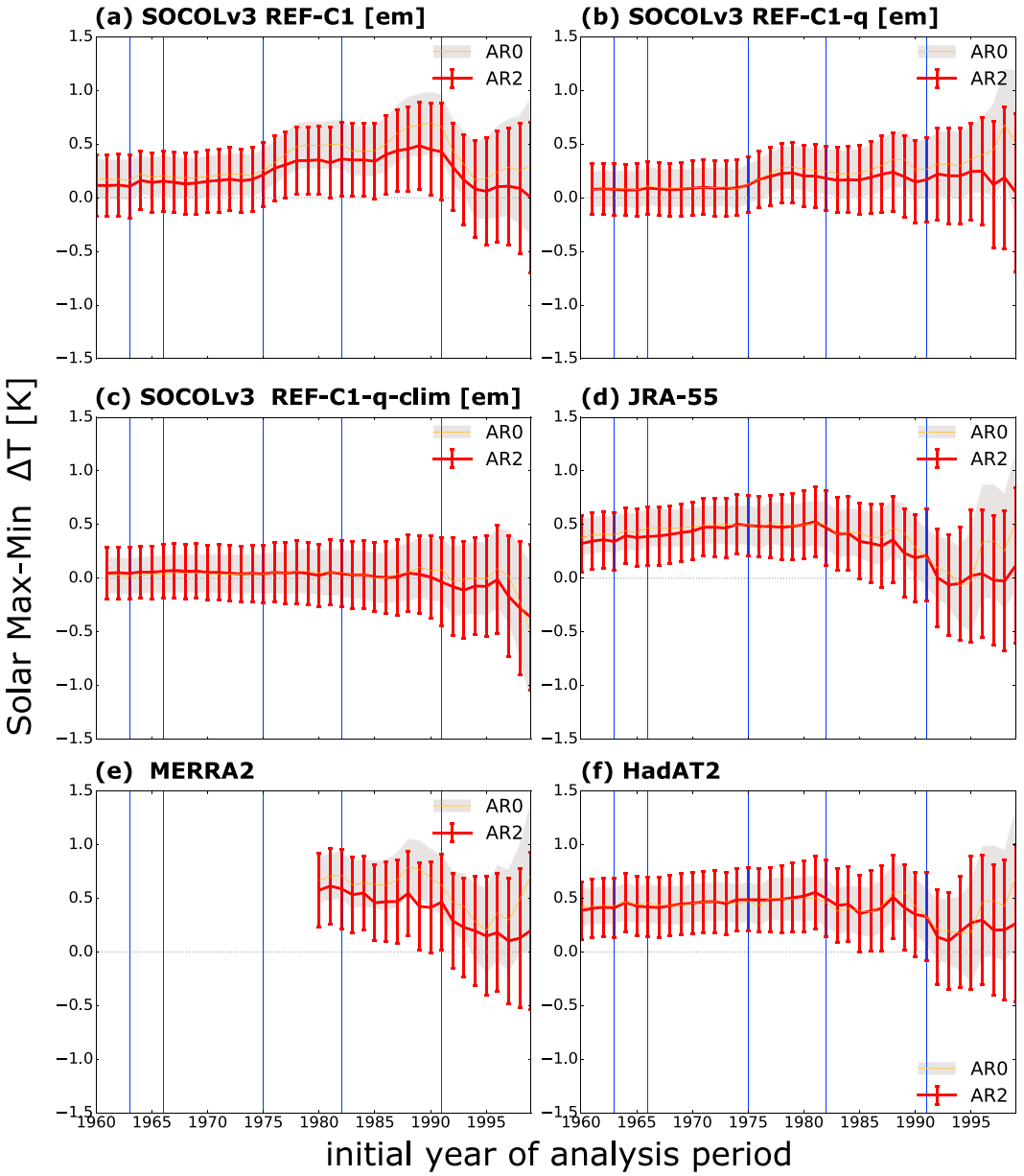

Figure 7. Tropical (25°S–25°N zonal mean) temperature response of various data sets or ensemble means (em) to $F_{10.7}$ at 50 hPa, when the initial year of the analysis is shifted backward in time and the ending year is fixed at 2009. Minimal analyzed period: 10 years, i.e., 1999–2009. Blue vertical lines: volcanic eruptions as labeled in Figure 1a. Vertical bars and shaded areas show the 95% confidence intervals, obtained with or without the AR2 residual model.

extracted in one depends partly on the other. Let us consider a simplified case where only $F_{10.7}$ and SAD regressors are included, such that

$$\mathrm{SAD}(t) = a + bF_{10.7}(t), \tag{2}$$

and the regression equation (1) is limited to solar and volcanic proxies. Then

$$Y(t) = \alpha^* + \gamma^* F_{10.7}(t) + e(t), \tag{3}$$

where $\alpha^* = (\alpha + a\beta)$ and $\gamma^* = (\gamma + b\beta)$. Finally, if $\beta > 0$, i.e., if there is a positive relationship between temperature and SAD, then there are three possibilities for b:

1. $b < 0$ represents a negative correlation between $F_{10.7}$ and SAD and $\gamma^* < \gamma$, i.e., the computed solar regression coefficient is underestimated.

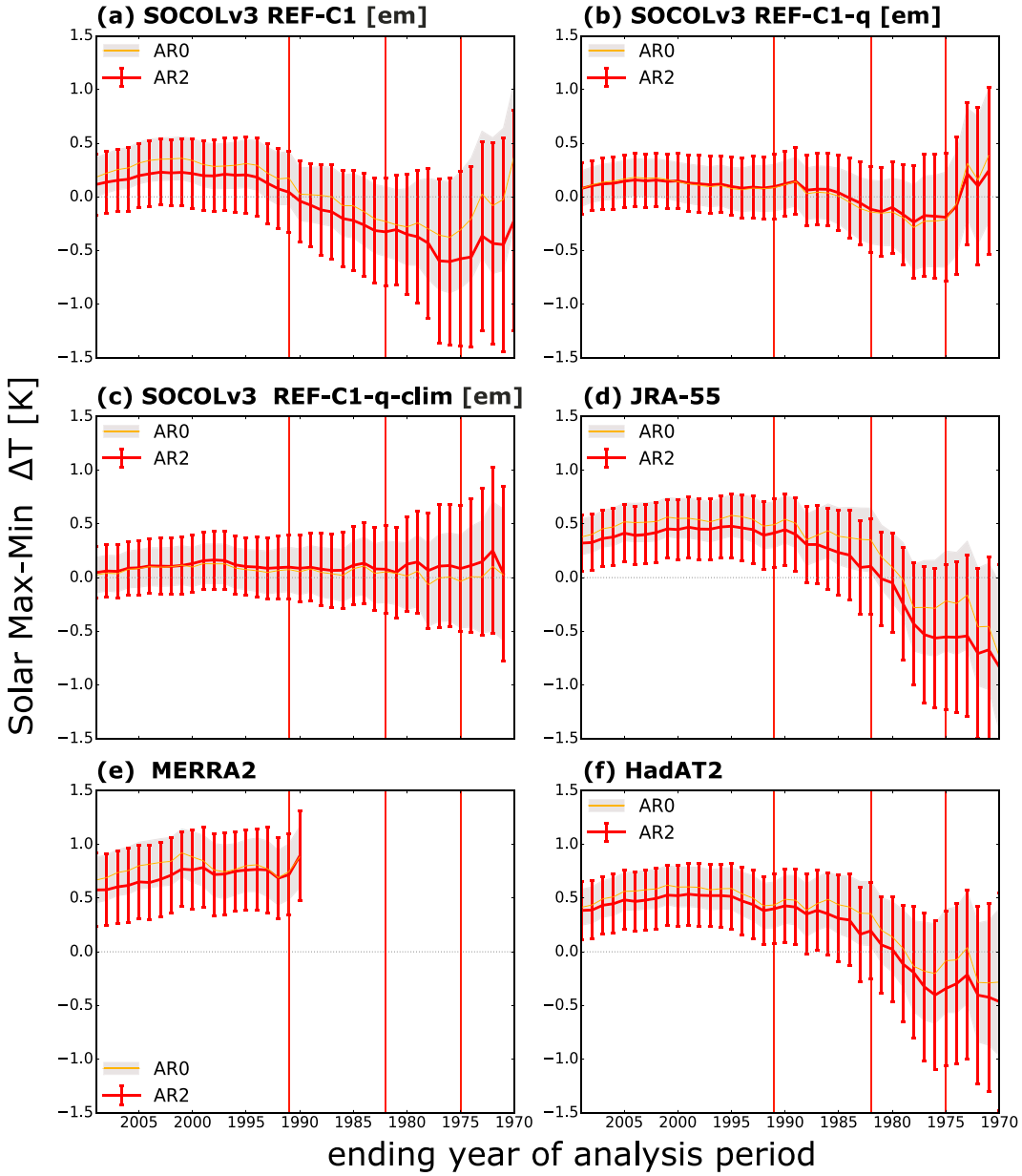

Figure 8. Tropical (25°S–25°N zonal mean) temperature response to $F_{10.7}$ at 50 hPa, when the ending year of the target period is shifted between 1970 and 2009, while the initial year is fixed at 1960 (minimal analyzed period: 10 years). Red vertical lines: volcanic eruptions as labeled in Figure 1a. Error bars and shaded areas represent the 95% confidence intervals when using AR2 residual model or without considering the residual autocorrelations (AR0), respectively.

2. $b > 0$ represents a positive correlation between $F_{10.7}$ and SAD and $\gamma^* > \gamma$, i.e., the computed solar regression coefficient is overestimated.
3. $b \sim 0$ represents no correlation between $F_{10.7}$ and SAD and $\gamma^* \sim \gamma$ (nonaliased regression coefficient).

Figure 6f shows the negative correlation ($b < 0$) for the periods after the Mount Pinatubo eruption, which gives an underestimated regression coefficient; in REF-C1 (Figure 7a) the mean value, although not negative, is at its lowest for the periods considered. On the other hand, in the periods between Mount Agung and Mount Pinatubo, we observe positive correlations ($b > 0$). This corresponds to the larger estimates of the temperature response (Figure 7), and, from above, this suggests that this would be an overestimate. Finally, if we consider periods in REF-C1 (Figure 7a) prior to 1966, long enough to eliminate the correlation between solar and volcanic proxies ($b \sim 0$), i.e., when El Chichón and Mount Pinatubo eruptions are aligned with solar

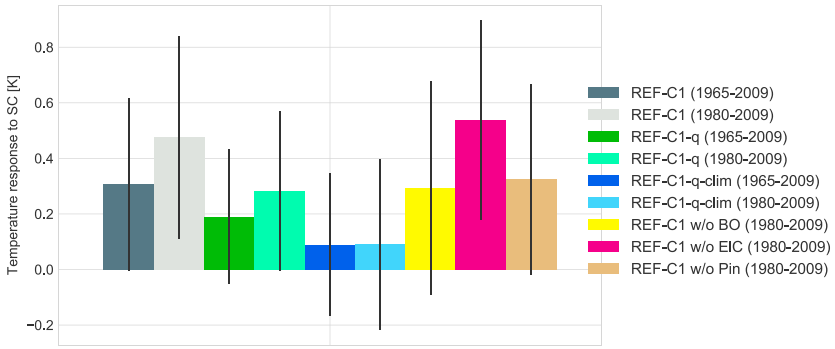

Figure 9. Tropical annual mean temperature response to the SC over the periods 1980–2009 and 1965–2009 at 30 hPa, where the tropical temperature response to volcanic eruptions maximizes (Figure 2b), in REF-C1 (gray bars), REF-C1-q (green bars), and REF-C1-q-clim (blue bars). In addition, the temperature response in REF-C1 over the period 1980–2009 was analyzed when years with particular volcanic eruptions, i.e., El Chichón (magenta bar; EIC) or Mount Pinatubo (tan bar; Pin), were removed individually or both at same time (yellow bar, BO).

maxima with the descending phase of solar maxima 21 and 22, the signal in temperature stabilizes and is in good agreement with REF-C1-q and REF-C1-q-clim (Figures 7b and 7c) where no volcanoes are present.

Figure 9 illustrates how the tropical annual mean temperature response to the SC changes at 30 hPa when years with either (BO) both El Chichón and Mount Pinatubo eruptions (yellow bar) or particular eruptions (magenta bar for El Chichón (EIC) or tan bar for Mount Pinatubo (Pin)) only were removed. The temperature response at in REF-C1 over the period 1980–2009 (dark gray bar) was reduced down to the temperature response over the period 1965–2009 (light gray bar). Note that we reach a similar value (∼0.3 K) in REF-C1-q over the period 1980–2009 (sea green bar) in comparison to REF-C1 over the period 1965–2009 and REF-C1 over the period 1980–2009 when years covering either or Mount Pinatubo, in particular, eruptions were removed. However, the temperature response over the period 1965–2009 (green bar) is slightly lower. These results show that the aliasing with the volcanic signal can be avoided either by removing years mainly with Mount Pinatubo or by analyzing a sufficiently long period to reach stable results. The temperature response is reduced further, down to ∼0.1 K, in REF-C1-q-clim (blue and light blue bars). This suggests that one is not able to remove the aliasing coming from SST/SIC variability.

Further overestimation in REF-C1 may stem from equation (2), where we assumed that $F_{10.7}$ and SAD are independent of other regressors. Note that the multicollinearity is rather a property of a set of regressors, not just a pair of them, i.e., that $F_{10.7}$ and SAD are also correlated with TREND and ENSO (as shown in Figures 6a and 6g, and 6b and 6j, respectively). The multicollinearity is projected into the solar signal through the volcanic aerosols and ENSO influence in the TLS, i.e., through volcanic and ENSO signatures operating in this region [*Mitchell et al.*, 2015a]. The same logic may be applied in the upper stratosphere where the long-term anthropogenic trend reveals even higher relative importance than the 11 year solar cycle variability [*Ball et al.*, 2016].

The autocorrelation modeling has already been examined by *Mitchell et al.* [2015b], comparing MLR results obtained with two different methods that treat autocorrelation in residuals and one without any residual modeling (AR0). The first method, developed by *Tiao et al.* [1990], corresponds to our regression model, i.e., modeling residuals as an autoregressive process. However, first-order autoregressive (AR1) modeling has been used in the study by *Mitchell et al.* [2015b], arguing that AR1 was sufficient and higher-order autoregressive processes did not change the significance of the results. The second method, following the Box-Jenkins prewhitening procedure [*Box*, 2012], was used by *Chiodo et al.* [2014]. The sensitivity test by *Mitchell et al.* [2015b] demonstrated that the Tiao method gives the most conservative estimate and shows that the Box-Jenkins method, as well as a setup without any residual modeling, may lead to an overconfident statistical significance.

In agreement with *Mitchell et al.* [2015b], we also found that the AR1 process occasionally sufficed to approximate the residual structure but only in the upper stratosphere (not shown). The differences between our results with AR0 and AR2 (corresponding to the Tiao method with second-order autoregressive modeling) in the lower stratosphere in Figures 7 for REF-C1 (a), REF-C1-q (b), and MERRA2 (d) and others considering very

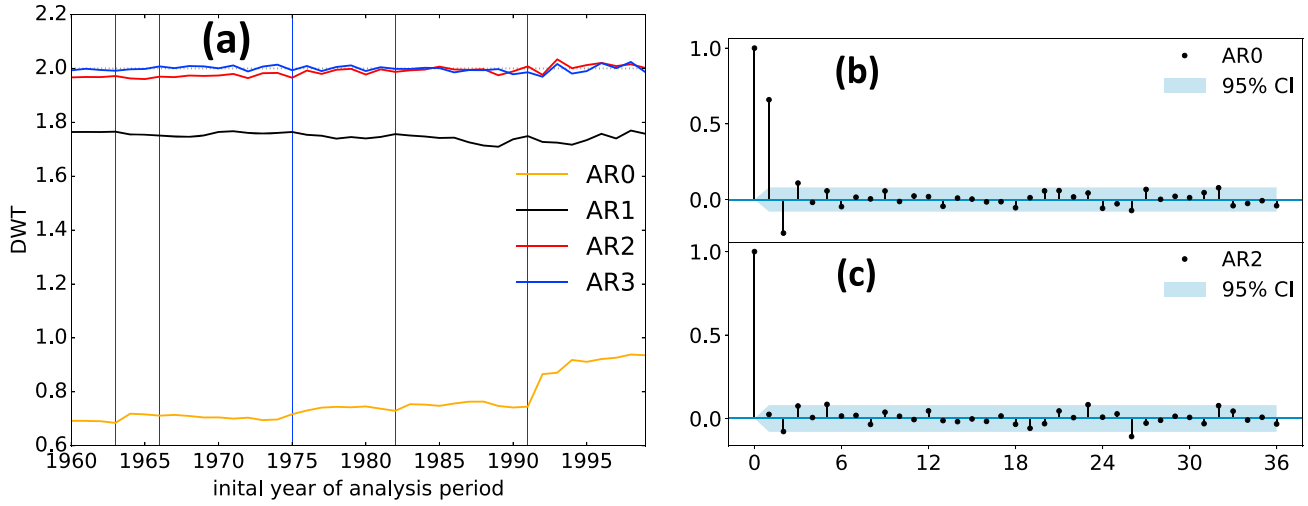

Figure 10. (a) Durbin-Watson test (DWT) [*Durbin and Watson*, 1950] of residuals from particular autoregressive residual models (AR) in regression analysis of REF-C1 tropical temperature time series at 50 hPa, for the analysis periods starting between 1960 and 1999 and ending at 2009 (minimal analyzed period: 10 years). Dotted gray line represents DWT = 2 indicating no autocorrelation. Partial autocorrelation function of residuals modeled as (b) AR0 and (c) AR2 for regression analysis of REF-C1 (em) tropical temperature time series at 50 hPa over the period 1965–2009.

short periods also demonstrate that the standard deviation of the solar regression coefficient is underestimated and the amplitude estimate may be biased as well. These findings are consistent with the statistical modeling literature [e.g., *Neter et al.*, 2004; *Thejll and Schmith*, 2005].

Figure 10a shows that AR1 removes most of the autocorrelation in residuals but not completely. This finding is in agreement with the study by *Ball et al.* [2016] concluding that AR1 was necessary but not sufficient. Furthermore, Figures 10a and 10b indicate that for periods prior to approximately 1975, AR3 would be able to completely remove the autocorrelation. However, the partial autocorrelation function in Figure 10c documents that the regression analysis with AR2 removes the autocorrelation from the residuals. While the radiative time scale in the lower stratosphere has been estimated to be between 30 to 100 days [*Randel et al.*, 2002; *Hood*, 2016], the radiative relaxation time scale in the upper stratosphere is around 10 days [*Mlynczak et al.*, 1999; *Brasseur and Solomon*, 2006]. While we cannot provide a robust physical explanation, these radiative time scales could hint at the physical explanation as to why the lower tropical stratosphere should be treated with a higher order of AR process.

5. Conclusions

Using the SOCOLv3 model and our own MLR-based tool called *X-regression* [*Kuchar*, 2016], we have characterized the tropical temperature variability to the 11 year SC. The upper stratospheric response in SOCOL reveals good agreement with SSU observations, but it is underestimated in comparison to the MERRA2 reanalysis. The origin of the systematic altitudinal difference of SC attribution in the TLS between SOCOL and MERRA2 reanalysis may be due to volcanic aerosol forcing data in the model. We discussed the sensitivity of our model to the prescribed aerosol boundary conditions compiled for CCMI and CMIP6 initiatives and conclude that SOCOLv3 with the CCMI aerosol forcing gives a overestimated temperature response to volcanic aerosols and possibly leads to an overestimated volcanic aliasing of the solar response. On the contrary, utilization of the new CMIP6 volcanic forcing removed this overestimation due to the volcanic aerosol heating effect during the Mount Agung and Pinatubo eruptions. Furthermore, the aliasing of the solar response was reduced in our short model experiments using the new CMIP6 volcanic forcing.

Using the SOCOL CCM sensitivity simulation REF-C1-q and statistical techniques such as wavelet analysis, in addition to MLR, we have shown that the fraction of the temperature response in the TLS attributable to the 11 year solar cycle is only about half of that found in previous studies analyzing model simulations [*Hood et al.*, 2015; *Mitchell et al.*, 2015b] or reanalyses [*Mitchell et al.*, 2015a] based on the periods coinciding with satellite measurements. This reduction is a result of removing the volcanic forcing from the time series and confirms the results of *Chiodo et al.* [2014], where a different CCM to SOCOLv3 was used.

The use of climatological SSTs/SICs, in addition to background stratospheric aerosols, completely removes volcanic and ENSO signals and almost entirely eliminates the lower stratospheric solar cycle signal. This highlights the crucial role of SST/SIC interannual variability in simulating the secondary maximum in the TLS. Therefore, we hypothesize that the SC attribution in REF-C1-q-clim represents the UV-induced changes in the upper stratosphere propagating downward, i.e., a separation from the non-UV-induced or other decadal-like changes in the surface propagating upward. These results may contribute to the discussion about how stratospheric temperature perturbations implied by the 11 year solar cycle propagate to the troposphere [*Mitchell et al.*, 2015b]. The fact that the annual temperature response to the SC in the TLS was not detected in the REF-C1-q-clim simulation implies that the temperature response in the TLS may be induced only in winter (being masked in the annual mean) by a weaker BDC [*Kodera and Kuroda*, 2002] and that the solar signal propagates downward via the equatorial route proposed by *Simpson et al.* [2009]. Or the signal may propagate via the polar route hypothesized by *Kodera* [2005] or through a combination of these two routes [*Kidston et al.*, 2015]. These hypotheses need further investigation.

Using our simulations and regression-based attribution to the SC, we showed that it is possible to provide robust estimates either by removing the years following strong volcanic events (recommended for data sets limited for example by the satellite observational era) or analyzing a sufficiently long period, such as 1965–2009 (recommended for analyses of climate model simulations). However, the resulting estimates are still largely impacted by the aliasing with SST/SIC variability.

We explain how a misattribution of another regressor to the solar signal may occur as a result of their collinearity, leading to aliasing. This incorrect attribution, in essence, leads to incorrect conclusions. Therefore, when using MLR without supporting model simulations, one needs to be concerned about the aliasing of the regressors and, consequently, about the proper choice of time period used for the attribution.

Finally, residual modeling is essential to properly determine the statistical significance and amplitude of the signals of interest. We demonstrate that the first-order autoregressive process (AR1) was necessary in our analyses but not sufficient to completely account for the residuals' autocorrelation, especially in the lower stratosphere, which was better represented with AR3. These issues are crucial for correct trend analysis or model validation based on the regression approach.

Acknowledgments

The authors would like to thank to the relevant working teams for the reanalysis: MERRA2 and JRA-55 and observation: SSU-AMSU, MSU/AMSU, and HadAT2. Furthermore, we acknowledge python open-source software libraries used for this paper for MLR: *statsmodels* [*Seabold and Perktold*, 2010]; data processing: *xarray* [*Hoyer and Hamman*, 2017], *pandas* [*McKinney*, 2010]; and visualization: *matplotlib* [*Hunter*, 2007], *seaborn* [*Waskom et al.*, 2016]. A.K. was supported by the Charles University, Grant Agency project1474314, the Czech Science Foundation (GA CR)16-01562J, and by the Swiss Government Excellence Scholarship, reference 2014.0190. E.R. was partially supported by the SNSF under grant agreement CRSII2-147659 (FUPSOL II). W.T.B. was supported by SNSF grants 200021-149182 (SILA) and 200020-163206 (SIMA). REF-C1-q, REF-C1-q-clim, and REF-C1-CMIP6aer zonally averaged temperature data sets are provided via the Mendeley Data portal [*Kuchar and Revell*, 2017]. The SOCOLv3 REF-C1 data set can be accessed through the Centre for Environmental Data Analysis [*Hegglin and Lamarque*, 2017].

References

Arfeuille, F., B. P. Luo, P. Heckendorn, D. Weisenstein, J. X. Sheng, E. Rozanov, M. Schraner, B. S., L. W. Thomason, and T. Peter (2013), Modeling the stratospheric warming following the Mt. Pinatubo eruption: Uncertainties in aerosol extinctions, *Atmos. Chem. Phys.*, *13*(22), 11,221–11,234, doi:10.5194/acp-13-11221-2013.

Austin, J., et al. (2008), Coupled chemistry climate model simulations of the solar cycle in ozone and temperature, *J. Geophys. Res.*, *113*, D11306, doi:10.1029/2007JD009391.

Ball, W. T., N. A. Krivova, Y. C. Unruh, J. D. Haigh, and S. K. Solanki (2014), A new SATIRE-S spectral solar irradiance reconstruction for solar cycles 21–23 and its implications for stratospheric ozone*, *J. Atmos. Sci.*, *71*(11), 4086–4101, doi:10.1175/JAS-D-13-0241.1.

Ball, W. T., et al. (2016), An upper-branch Brewer-Dobson circulation index for attribution of stratospheric variability and improved ozone and temperature trend analysis, *Atmos. Chem. Phys.*, *2016*, 1–20, doi:10.5194/acp-2016-449.

Box, G. (2012), Box and Jenkins: Time series analysis, forecasting and control, in *A Very British Affair: Six Britons and the Development of Time Series Analysis During the 20th Century*, pp. 161–215, Palgrave Macmillan, London.

Brasseur, G. P., and S. Solomon (2006), *Aeronomy of the Middle Atmosphere: Chemistry and Physics of the Stratosphere and Mesosphere*, vol. 32, Springer, Netherlands.

Bretherton, C. S., M. Widmann, V. P. Dymnikov, J. M. Wallace, and I. Bladé (1999), The effective number of spatial degrees of freedom of a time-varying field, *J. Clim.*, *12*(7), 1990–2009.

CCMVal, S. (2010), SPARC CCMVal Report on the Evaluation of Chemistry-Climate Models, in *SPARC Report*, vol. 5, edited by V. Eyring, T. G. Shepherd, and D. W. Waugh, 426 pp., SPARC Office. [Available at http://www.sparc-climate.org/publications/sparc-reports/.]

Chen, Y., Y. Han, Q. Liu, P. Van Delst, and F. Weng (2011), Community radiative transfer model for stratospheric sounding unit, *J. Atmos. Oceanic Technol.*, *28*(6), 767–778.

Chiodo, G., D. Marsh, R. Garcia-Herrera, N. Calvo, and J. García (2014), On the detection of the solar signal in the tropical stratosphere, *Atmos. Chem. Phys.*, *14*(11), 5251–5269.

Compo, G. P., et al. (2011), The twentieth century reanalysis project, *Q. J. R. Meteorol. Soc.*, *137*(654), 1–28, doi:10.1002/qj.776.

Dee, D. P., et al. (2011), The ERA-Interim reanalysis: Configuration and performance of the data assimilation system, *Q. J. R. Meteorol. Soc.*, *137*(656), 553–597.

Durbin, J., and G. S. Watson (1950), Testing for serial correlation in least squares regression: I, *Biometrika*, *37*, 409–428.

Ebita, A., et al. (2011), The Japanese 55-year reanalysis (JRA-55): An interim report, *Sola*, *7*, 149–152.

Egorova, T., E. Rozanov, V. Zubov, and I. Karol (2003), Model for investigating ozone trends (MEZON), *Izvestiya Atmos. Oceanic Phys.*, *39*(3), 277–292.

Egorova, T., E. Rozanov, E. Manzini, M. Haberreiter, W. Schmutz, V. Zubov, and T. Peter (2004), Chemical and dynamical response to the 11-year variability of the solar irradiance simulated with a chemistry-climate model, *Geophys. Res. Lett.*, *31*, L06119, doi:10.1029/2003GL019294.

Ermolli, I., et al. (2013), Recent variability of the solar spectral irradiance and its impact on climate modelling, *Atmos. Chem. Phys.*, *13*(8), 3945–3977, doi:10.5194/acp-13-3945-2013.

Eyring, V., et al. (2014), Report on the IGAC/SPARC Chemistry-Climate Model Initiative (CCMI) 2013 science workshop, in *Report on the 34th Session of the Joint Scientific Committee of the World Climate Research Programme*, p. 23.
Frame, T. H. A., and L. J. Gray (2010), The 11-yr solar cycle in ERA-40 data: An update to 2008, *J. Clim.*, *23*(8), 2213–2222, doi:10.1175/2009JCLI3150.1.
Fujiwara, M., T. Hibino, S. K. Mehta, L. Gray, D. Mitchell, and J. Anstey (2015), Global temperature response to the major volcanic eruptions in multiple reanalysis datasets, *Atmos. Chem. Phys. Discuss.*, *15*(9), 13,315–13,346, doi:10.5194/acpd-15-13315-2015.
Giorgetta, M. A., E. Manzini, E. Roeckner, M. Esch, and L. Bengtsson (2006), Climatology and forcing of the quasi-biennial oscillation in the MAECHAM5 model, *J. Clim.*, *19*(16), 3882–3901, doi:10.1175/JCLI3830.1.
Gray, L. J., et al. (2010), Solar influences on climate, *Rev. Geophys.*, *48*, RG4001, doi:10.1029/2009RG000282.
Gray, L. J., A. A. Scaife, D. M. Mitchell, S. Osprey, S. Ineson, S. Hardiman, N. Butchart, J. Knight, R. Sutton, and K. Kodera (2013), A lagged response to the 11 year solar cycle in observed winter Atlantic/European weather patterns, *J. Geophys. Res. Atmos.*, *118*(24), 13,405–13,420, doi:10.1002/2013JD020062.
Hegglin, I. M., and J. F. Lamarque (2017), The IGAC/SPARC Chemistry-Climate Model Initiative phase-1 (CCMI-1) model data output. NCAS British Atmospheric Data Centre. [Available at http://catalogue.ceda.ac.uk/uuid/9cc6b94df0f4469d8066d69b5df879d5.]
Hood, L. (2016), Lagged response of tropical tropospheric temperature to solar ultraviolet variations on intraseasonal time scales, *Geophys. Res. Lett.*, *43*, 4066–4075, doi:10.1002/2016GL068855.
Hood, L. L., and B. E. Soukharev (2012), The lower-stratospheric response to 11-yr solar forcing: Coupling to the troposphere-ocean response, *J. Atmos. Sci.*, *69*(6), 1841–1864, doi:10.1175/JAS-D-11-086.1.
Hood, L. L., et al. (2015), Solar signals in CMIP-5 simulations: The ozone response, *Q. J. R. Meteorol. Soc.*, *141*, 2670–2689, doi:10.1002/qj.2553.
Hoyer, S., and J. Hamman (2017), Xarray: N-D labeled Arrays and Datasets in Python, *J. Open Res. Softw.*, *5*(1).
Hunter, J. D. (2007), Matplotlib: A 2D graphics environment, *Comput. Sci. Eng.*, *9*(3), 90–95.
Kalnay, E., et al. (1996), The NCEP/NCAR 40-year reanalysis project, *Bull. Am. Meteorol. Soc.*, *77*(3), 437–471, doi:10.1175/1520-0477(1996)077<0437:TNYRP>2.0.CO;2.
Kidston, J., A. A. Scaife, S. C. Hardiman, D. M. Mitchell, N. Butchart, M. P. Baldwin, and L. J. Gray (2015), Stratospheric influence on tropospheric jet streams, storm tracks and surface weather, *Nat. Geosci.*, *8*, 433–440, doi:10.1038/ngeo2424.
Kodera, K. (2005), A possible mechanism of solar modulation of the spatial structure of the North Atlantic Oscillation, *J. Geophys. Res.*, *110*, D02111, doi:10.1029/2004JD005258.
Kodera, K., and Y. Kuroda (2002), Dynamical response to the solar cycle, *J. Geophys. Res.*, *107*(D24), 5–12, doi:10.1029/2002JD002224.
Koster, R. D., et al., (2015), Technical report series on global modeling and data assimilation, volume 43. MERRA-2; initial evaluation of the climate., Tech. Rep. NASA/TM-2015-104606/VOL.43, GSFC-E-DAA-TN29739, NASA Goddard Space Flight Center, Greenbelt, Md.
Krivova, N. A., L. E. A. Vieira, and S. K. Solanki (2010), Reconstruction of solar spectral irradiance since the maunder minimum, *J. Geophys. Res.*, *115*, A12112, doi:10.1029/2010JA015431.
Kuchar, A. (2016), kuchaale/X-regression: X-regression: First release kuchaale/X-regression: X-regression: First release, doi:10.5281/zenodo.159817.
Kuchar, A., and L. Revell (2017), Model simulations data to "on the aliasing of the solar cycle in the lower-stratospheric tropical temperature," Mendeley data, doi:10.17632/khrhbw6wn5.1.
Kuchar, A., P. Sacha, J. Miksovsky, and P. Pisoft (2015), The 11-year solar cycle in current reanalyses: A (non)linear attribution study of the middle atmosphere, *Atmos. Chem. Phys.*, *15*(12), 6879–6895, doi:10.5194/acp-15-6879-2015.
Lean, J., G. Rottman, J. Harder, and G. Kopp (2005), Sorce contributions to new understanding of global change and solar variability, in *The Solar Radiation and Climate Experiment (SORCE)*, pp. 27–53, Springer, New York.,10.1007/0-387-37625-9_3
Lee, H., and A. K. Smith (2003), Simulation of the combined effects of solar cycle, quasi-biennial oscillation, and volcanic forcing on stratospheric ozone changes in recent decades, *J. Geophys. Res.*, *108*, 4049, doi:10.1029/2001JD001503.
Luo, B. P. (2013), Ccmi aerosol data set, ETH, Zurich. [Available at ftp://iacftp.ethz.ch/pub_read/luo/ccmi/, last accessed 1 Nov 2015.
Luo, B. P. (2016), CMIP6 aerosol data set, ETH, Zurich. [Available ftp://iacftp.ethz.ch/pub_read/luo/CMIP6/, last accessed 1 Nov 2016].
Manzini, E., M. Giorgetta, M. Esch, L. Kornblueh, and E. Roeckner (2006), The influence of sea surface temperatures on the northern winter stratosphere: Ensemble simulations with the MAECHAM5 model, *J. Clim.*, *19*(16), 3863–3881.
Marsh, D. R., and R. R. Garcia (2007), Attribution of decadal variability in lower-stratospheric tropical ozone, *Geophys. Res. Lett.*, *34*(21), doi:10.1029/2007GL030935.
Marsh, D. R., R. R. Garcia, D. E. Kinnison, B. A. Boville, F. Sassi, S. C.Solomon, and K. Matthes (2007), Modeling the whole atmosphere response to solar cycle changes in radiative and geomagnetic forcing, *J. Geophys. Res.*, *112*, D23306, doi:10.1029/2006JD008306.
Matthes, K., K. Kodera, R. R. Garcia, Y. Kuroda, D. R. Marsh, and K. Labitzke (2013), The importance of time-varying forcing for QBO modulation of the atmospheric 11 year solar cycle signal, *J. Geophys. Res. Atmos.*, *118*(10), 4435–4447, doi:10.1002/jgrd.50424.
Matthes, K., et al. (2016), Solar forcing for CMIP6 (v3.1), *Geosci. Model Dev. Discuss.*, *10*, 2247–2302, doi:10.5194/gmd-2016-91.
McKinney, W. (2010), Data structures for statistical computing in python, in *Proceedings of the 9th Python in Science Conference*, edited by S. van der Walt and and J. Millman, pp. 51–56. [Available at http://conference.scipy.org/proceedings/scipy2010/mckinney.html.]
McLandress, C., D. A. Plummer, and T. G. Shepherd (2014), Technical note: A simple procedure for removing temporal discontinuities in ERA-interim upper stratospheric temperatures for use in nudged Chemistry-Climate Model simulations, *Atmos. Chem. Phys.*, *14*(3), 1547–1555, doi:10.5194/acp-14-1547-2014.
Mears, C. A., and F. J. Wentz (2009), Construction of the remote sensing systems v3. 2 atmospheric temperature records from the MSU and AMSU microwave sounders, *J. Atmos. Oceanic Technol.*, *26*(6), 1040–1056.
Mitchell, D. M., L. J. Gray, M. Fujiwara, T. Hibino, J. A. Anstey, W. Ebisuzaki, Y. Harada, C. Long, S. Misios, P. A. Stott, and D. Tan (2015a), Signatures of naturally induced variability in the atmosphere using multiple reanalysis datasets, *Q. J. R. Meteorol. Soc.*, *141*(691), 2011–2031, doi:10.1002/qj.2492.
Mitchell, D. M., et al. (2015b), Solar signals in CMIP-5 simulations: The stratospheric pathway, *Q. J. R. Meteorol. Soc.*, *141*, 2390–2403, doi:10.1002/qj.2530.
Mlynczak, M. G., C. J. Mertens, R. R. Garcia, and R. W. Portmann (1999), A detailed evaluation of the stratospheric heat budget: 2. Global radiation balance and diabatic circulations, *J. Geophys. Res.*, *104*(D6), 6039–6066, doi:10.1029/1998JD200099.
Morgenstern, O., et al. (2017), Review of the global models used within phase 1 of the Chemistry-Climate Model Initiative (CCMI), *Geosci. Model Dev.*, *10*(2), 639–671, doi:10.5194/gmd-10-639-2017.
Muthers, S., A. Kuchar, A. Stenke, J. Schmitt, J. G. Anet, C. C. Raible, and T. F. Stocker (2016), Stratospheric age of air variations between 1600 and 2100, *Geophys. Res. Lett.*, *43*, 5409–5418, doi:10.1002/2016GL068734.
Neter, J., M. Kutner, W. Wasserman, and C. Nachtsheim (2004), *Applied Linear Statistical Models*, 5th ed., McGraw-Hill Irwin, New York.

Randel, W. J., R. R. Garcia, and F. Wu (2002), Time-dependent upwelling in the tropical lower stratosphere estimated from the zonal-mean momentum budget, *J. Atmos. Sci.*, *59*(13), 2141–2152, doi:10.1175/1520-0469(2002)059<2141:TDUITT>2.0.CO;2.

Randel, W. J., et al. (2009), An update of observed stratospheric temperature trends, *J. Geophys. Res.*, *114*, D02107, doi:10.1029/2008JD010421.

Rayner, N., D. E. Parker, E. Horton, C. Folland, L. Alexander, D. Rowell, E. Kent, and A. Kaplan (2003), Global analyses of sea surface temperature, sea ice, and night marine air temperature since the late nineteenth century, *J. Geophys. Res.*, *108*(D14), 4407, doi:10.1029/2002JD002670.

Revell, L. E., F. Tummon, A. Stenke, T. Sukhodolov, A. Coulon, E. Rozanov, H. Garny, V. Grewe, and T. Peter (2015), Drivers of the tropospheric ozone budget throughout the 21st century under the medium-high climate scenario RCP 6.0, *Atmos. Chem. Phys.*, *15*(10), 5887–5902, doi:10.5194/acp-15-5887-2015.

Revell, L., A. Stenke, B. Luo, S. Kremser, E. Rozanov, T. Sukhodolov, and T. Peter (2017), Chemistry-climate model simulations of the Mt. Pinatubo eruption using CCMI and CMIP6 stratospheric aerosol data, *Atmos. Chem. Phys. Discuss.*, *2017*, 1–17, doi:10.5194/acp-2017-633.

Rienecker, M. M., et al. (2011), MERRA: NASA's Modern-Era Retrospective Analysis for Research and Applications, *J. Clim.*, *24*(14), 3624–3648.

Seabold, S., and J. Perktold (2010), Statsmodels: Econometric and statistical modeling with python, in *Proceedings of the 9th Python in Science Conference*. [Available at https://conference.scipy.org/proceedings/scipy2010/pdfs/seabold.pdf.]

Simpson, I. R., M. Blackburn, and J. D. Haigh (2009), The role of eddies in driving the tropospheric response to stratospheric heating perturbations, *J. Atmos. Sci.*, *66*(5), 1347–1365.

Smith, A. K., and K. Matthes (2008), Decadal-scale periodicities in the stratosphere associated with the solar cycle and the QBO, *J. Geophys. Res.*, *113*, D05311, doi:10.1029/2007JD009051.

Stenke, A., M. Schraner, E. Rozanov, T. Egorova, B. Luo, and T. Peter (2013), The SOCOL version 3.0 chemistry climate model: Description, evaluation, and implications from an advanced transport algorithm, *Geosci. Model Dev.*, *6*(5), 1407–1427, doi:10.5194/gmd-6-1407-2013.

Thejll, T., and P. Schmith (2005), Limitations on regression analysis due to serially correlated residuals: Application to climate reconstruction from proxies, *J. Geophys. Res.*, *110*, D18103, doi:10.1029/2005JD005895.

Thorne, P. W., D. E. Parker, S. F. Tett, P. D. Jones, M. McCarthy, H. Coleman, and P. Brohan (2005), Revisiting radiosonde upper air temperatures from 1958 to 2002, *J. Geophys. Res.*, *110*, D18105, doi:10.1029/2004JD005753.

Tiao, G. C., G. C. Reinsel, D. Xu, J. H. Pedrick, X. Zhu, A. J. Miller, J. J. DeLuisi, C. L. Mateer, and D. J. Wuebbles (1990), Effects of autocorrelation and temporal sampling schemes on estimates of trend and spatial correlation, *J. Geophys. Res.*, *95*(D12), 20,507–20,517, doi:10.1029/JD095iD12p20507.

Torrence, C., and G. P. Compo (1998), A practical guide to wavelet analysis, *Bull. Am. Meteorol. Soc.*, *79*(1), 61–78.

Vernier, J.-P., et al. (2011), Major influence of tropical volcanic eruptions on the stratospheric aerosol layer during the last decade, *Geophys. Res. Lett.*, *38*, L12807, doi:10.1029/2011GL047563.

Wang, W., K. Matthes, N.-E. Omrani, and M. Latif (2016), Decadal variability of tropical tropopause temperature and its relationship to the Pacific Decadal Oscillation, *Sci. Rep.*, *6*, 29537, doi:10.1038/srep29537.

Waskom, M., et al. (2016), Seaborn: v0.7.1 (June 2016), doi:10.5281/zenodo.54844.

Yeo, K. L., N. A. Krivova, S. K. Solanki, and K. H. Glassmeier (2014), Reconstruction of total and spectral solar irradiance from 1974 to 2013 based on KPVT, SOHO/MDI, and SDO/HMI observations, *Astron. Astrophys.*, *570*, A85, doi:10.1051/0004-6361/201423628.

Zou, C.-Z., and H. Qian (2016), Stratospheric temperature climate data record from merged SSU and AMSU-A observations, *J. Atmos. Oceanic Technol.*, *33*, 1967–1984, doi:10.1175/JTECH-D-16-0018.1.